SPANDIDOS PUBLICATIONS

# Actin reorganization in CHO AA8 cells undergoing mitotic catastrophe and apoptosis induced by doxorubicin

D. GRZANKA[1], A. GRZANKA[2], M. IZDEBSKA[2], L. GACKOWSKA[3], A. STEPIEN[2] and A. MARSZALEK[1,4]

[1]Department of Clinical Pathomorphology, Collegium Medicum in Bydgoszcz, Nicolaus Copernicus University, Sklodowskiej-Curie 9, 85-094 Bydgoszcz; [2]Department of Histology and Embryology, Collegium Medicum in Bydgoszcz, Nicolaus Copernicus University, Karlowicza 24, 85-092 Bydgoszcz; [3]Department of Immunology, Collegium Medicum in Bydgoszcz, Nicolaus Copernicus University, Sklodowskiej-Curie 9, 85-094 Bydgoszcz; [4]Department of Clinical Pathomorphology, Poznan University of Medical Sciences, Przybyszewskiego 49, 60-355 Poznan, Poland

Received July 24, 2009; Accepted September 29, 2009

DOI: 10.3892/or_00000681

**Abstract.** Doxorubicin (DOX) is a drug widely used in cancer chemotherapy. Although it has been proven that DOX kills tumor cells, the triggered modes of cell death are not fully understood. There is some evidence that, depending on the dose of DOX, the treated cells undergo senescence, mitotic catastrophe, apoptosis or necrosis. The aim of this study was to assess the type of CHO AA8 cell death induced with different DOX doses. In this context, we also assessed organization and distribution of F-actin, which integrity was suggested to be indispensable for apoptosis. Following treatment with 0.5 and 1 $\mu$M DOX, the giant multinucleated cells with extended network of fine microfilaments appeared. Notably, in the nuclei of the enlarged cells microscopy and cytometric analysis showed the presence of F-actin. DOX (2.5 $\mu$M) caused the appearance of the giant cells and with apoptotic features and signs of autophagy vacuolization. Flow cytometric studies indicated a dose-dependent increase in the number of TUNEL-positive cells and cells stained with both Annexin V and PI. Cell cycle analysis revealed the increase in the hyperploid DNA content. Our results suggest that treatment of CHO AA8 cells with different DOX doses caused mitotic catastrophe that was followed by apoptosis with signs of autophagy. The increase in F-actin content in the nuclei of the dying cells was evident. We hypothesize that in CHO AA8 cells F-actin may be involved in chromatin reorganization undergoing cell death.

## Introduction

Doxorubicin (DOX) is the anthracycline antibiotic widely used in the treatment of solid tumors (1). Despite the widespread clinical application, the mechanism of action of DOX is not entirely clear. Its main activity is related to the inhibition of topoisomerase II, free radical formation and oxidative DNA damage (2,3). It is believed that DOX induces apoptosis through cytochrome c release and activation of caspase-3 (4,5). However, in our previous study we observed the occurrence of cells not only with apoptotic features, but those characteristic of mitotic catastrophe (6). Several lines of evidence have indicated that high doses of DOX cause cell death via apoptosis whereas low concentrations lead to mitotic catastrophe (MC) and/or senescence (7,8). The definition of MC is still the subject of debate. Castedo *et al* proposed this process to be different from apoptosis mode of cell death resulting from cell cycle checkpoint deficiencies and cellular damage (9). On the contrary, others have claimed that MC should be considered an aberrant mitosis that promotes autophagy (10) and/or leads to cell death through apoptosis, or necrosis (11,12). In spite of many discrepancies, it is believed that p53-deficient cells are particularly susceptible to MC. The hallmarks of MC include formation of the multinuclear giant cells with uncondensed chromosomes, multipolar spindle and polyploidy (13). Unlike MC, apoptosis is characterized by cell shrinkage, plasma membrane blebbing and nuclear fragmentation (14). Autophagy serves, depending on circumstances, as an adaptive process or a form of distinct cell death, among others, it is demonstrated by accumulation of multiple autophagy vesicles (15).

Actin is an abundant cytoskeletal protein present in all eucaryotic cells in two forms: globular actin (G-actin) and filamentous actin (F-actin) (16). Its activity is crucial in regulating signal transduction, membrane trafficking, polarity and motility of cells (17). It has been reported that actin might be both an apoptotic target and an early modulator of cell commitment to apoptosis (18). Moreover, reorganization of the actin network was proved to be required for plasma membrane blebbing (19,20). There is growing evidence that intact F-actin is required for autophagocytosis, presumably for enabling cells to transport vacuoles to lysosomes (21,22). Recent evidence has indicated that the undamaged actin filaments are also necessary for nuclear disruption during apoptosis (23). In our

*Correspondence to:* Dr D. Grzanka, Department of Clinical Pathomorphology, Collegium Medicum in Bydgoszcz, Nicolaus Copernicus University, Sklodowskiej-Curie 9, 85-094 Bydgoszcz, Poland
E-mail: d_gr@wp.pl

*Key words:* actin, mitotic catastrophe, apoptosis, CHO AA8

previous studies, we showed actin's presence in the nuclei of different cell lines treated with various cytostatic drugs including DOX (6,24). There are reports on the existence of actin in interphase nuclei (25,26). It is assumed that nuclear actin binds some structural proteins within the nucleus (27). It is also implicated in chromatin remodeling, gene transcription and pre-mRNA export (28-30).

In spite of some evidence, the presence of actin in nuclei of the living and dying cells, its polymeric state and possible function still remains controversial. Therefore, we decided to assess the mode of CHO AA8 cell death and changes in actin organization induced by different DOX doses.

## Materials and methods

*Cell culture and treatment*. Chinese hamster ovary cells (CHO AA8) were kindly provided by Professor M.Z. Zdzienicka from Department of Molecular Cell Genetics, Collegium Medicum in Bydgoszcz, Nicolaus Copernicus University, Poland. The cells were grown as adherent cultures on plastic in minimum essential medium eagle (MEM; Sigma Aldrich) supplemented with 10% foetal bovine serum (Gibco) and 10 ml/l antibiotic-antimycotic stabilized solution (penicillin, streptomycin, amphotericin B; Sigma Aldrich) in 5% $CO_2$ at 37˚C.

For induction of cell death, CHO AA8 cells were treated with different DOX concentrations: 0.5, 1 and 2.5 $\mu$M for 24 h. After this time period, the medium containing indicated DOX concentrations was replaced with drug-free medium. The cells were cultured for another 48 h period in fresh medium. Control cells were grown in the same conditions except for DOX treatment.

*The isolation of nuclei*. The cell pellet was suspended in the homogenizing solution: 0.5 M Tris-HCl (pH 7.5); 0.5 M $CaCl_2$; 1 M saccharose; 0.5 M $MgCl_2$; Nonidet, 2-mercaptoethanol. The solution-suspension ratio was 5:1. Homogenate was crushed with Teflon piston in glass homogenizer on ice, transferred into centrifugal tubes and centrifuged at 700 x g for 10 min, at 2˚C. Afterwards, cell precipitation was suspended in 1 ml of the homogenizing solution (without Nonidet) and slowly added to the cooled solution: 0.5 M Tris-HCl (pH 7.5); 0.5 M KCl; 1 M saccharose; glycerol; 0.5 $MgCl_2$ and 2-mercaptoethanol. The mixture was centrifuged at 700 x g for 10 min, at 2˚C. Finally, the supernatant was carefully decanted and precipitation was suspended in 1 ml of fixing solution [4% (v/v) PFA in PBS, pH 7.4].

*Fluorescence microscopy*. CHO AA8 cells were grown on sterile glass coverslips (Menzel) for the indicated time. For immunofluorescence analysis, the cells were fixed with 4% paraformaldehyde (PFA) in PBS, pH 7.4 (20 min, RT) and then stained for F-actin with phalloidin/Alexa Fluor 488 (Molecular Probes) in PBS containing 20% methanol (20 min, RT). Cell nuclei were stained with DAPI (Sigma Aldrich). Labeled cells were observed with an Eclipse E800 fluorescence microscope with Epi-fluorescence attachment (Nikon) and Confocal laser scanning microscopy Eclipse C1 (Nikon).

*Transmission electron microscopy*. For conventional transmission electron microscopy analysis, cells were fixed with 3.6% glutaraldehyde in phosphate buffer, postfixed with $OsO_4$ in the same buffer, dehydratated with alcohol and finally embedded in Epon 812. Thin sections were stained with uranyl acetate and lead citrate.

To show the presence of actin at the ultrastructural level, a post-embedding streptavidin gold method was used. CHO AA8 cells were fixed (4% PFA/PBS, 1 h, 4˚C) and washed overnight (PBS, 4˚C). The cells were dehydrated with graded ethanols and embedded in LR White. Sections were cut and placed on nickel grids (Sigma Aldrich). Afterwards the grids were floated on a drop of non-immune rabbit serum (Dako) for 20 min, transferred onto drops of 1:100 dilution of a monoclonal anti-actin antibody for 30 min (AC-40, Sigma Aldrich) and washed in PBS. After PBS rinse, grids were exposed to biotinylated rabbit anti-mouse immunoglobins (1:100 dilution) (Dako), washed in PBS and transferred onto drops of 1:20 dilution of 10 nm gold particles conjugated to streptavidin for 30 min (Sigma Aldrich). Finally, the grids were rinsed in PBS and dried. Control specimens were incubated with non-imune anti-serum (Dako). All preparations were examined in a JEM 100 CX electron microscope (Jeol, Tokyo, Japan) at 80 kV.

*Flow cytometry*

*Annexin V-FITC assay*. Annexin V-FITC apoptosis detection kit (BD Pharmingen) was used to assess phosphatidylserine externalization. Nuclei were counterstained with propidium iodide. The assay was performed according to manufacturer's instruction. For flow cytometric analyses the Becton-Dickinson FACScan was used.

*TUNEL assay*. The TUNEL (terminal deoxynucleotidyl transferase-mediated dUTP-biotin nick end-labeling) method was used to detect DNA strand breaks. TUNEL was carried out according to manufacturer's instruction, with the following modifications: cell fixation was performed on ice (15 min, 1% formaldehyde) and was followed by cell permeabilization in 70% ethanol (30 min, on ice). After TUNEL-FITC staining, the propidium iodide (PI)/RNase solution was added to detect the stage of cell cycle. Analyses were performed on a Becton-Dickinson FACScan machine.

For the analysis of DNA content, doublets were excluded from the final analysis using linear plots of FL2-A vs. FL2-W. The fractions of cells in G0/G1, S, G2/M, cells with a DNA content of >4 n and <2 n (apoptotic DNA) were indentified. Data analysis was carried out using FlowJo cell cycle analysis software (Tree Star).

*F-actin content*. CHO AA8 cells were fixed with 4% PFA for 20 min, at 4˚C and washed with PBS. Then the cells were permeabilized with 0.1% Triton X-100 for 3 min, rinsed with PBS and stained with phalloidin/Alexa Fluor 488, 20 min, RT (Molecular Probes). Flow cytometric evaluation of DNA content was performed using Becton-Dickinson FACScan.

*Statistical analysis*. Quantitative experiments were analyzed by Mann-Whitney U test. Results were considered significant

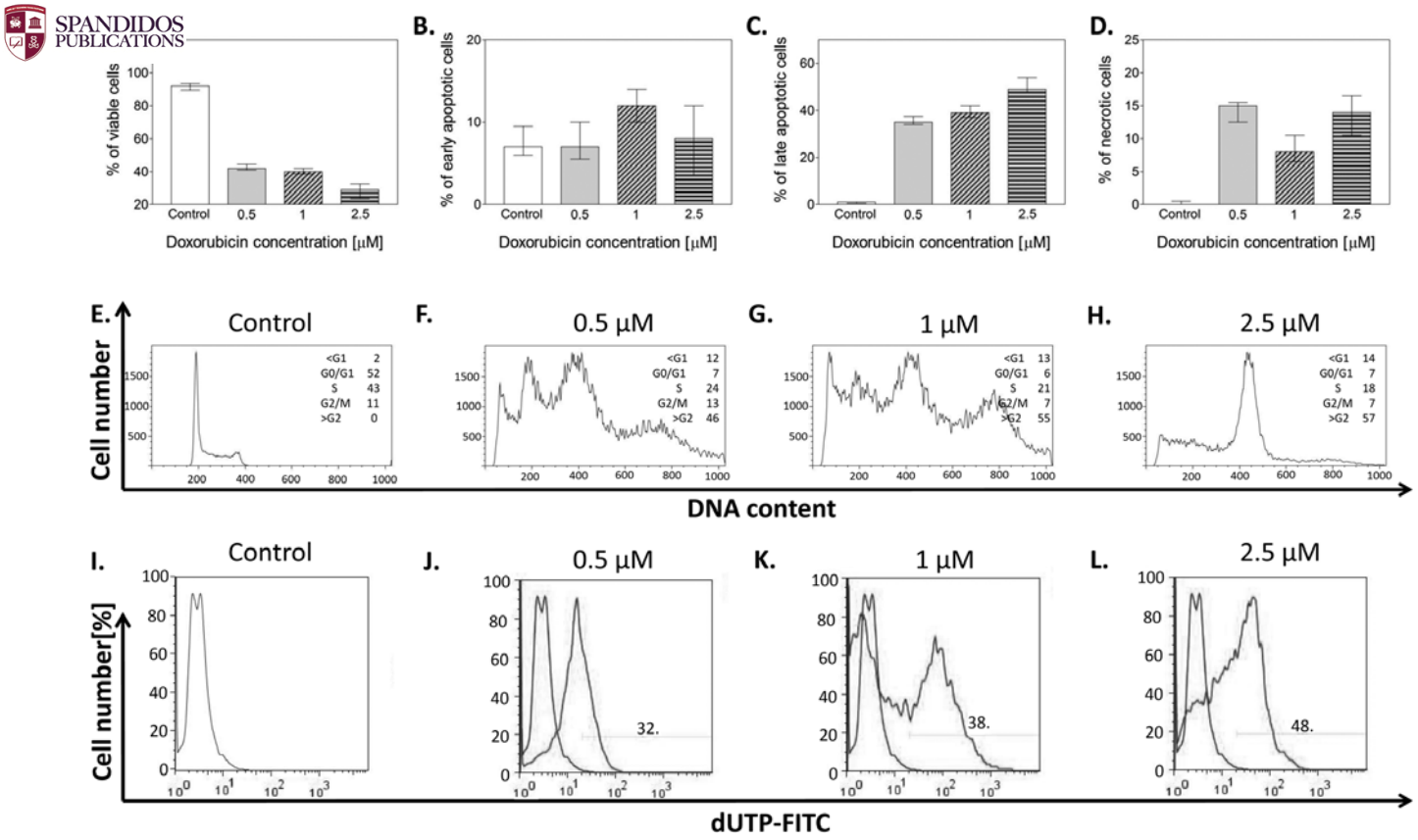


Figure 1. Flow cytometry analysis of viable (A), early apoptotic (B), late apoptotic (C) and necrotic cells (D) in relation to control cells. The CHO AA8 cells are double-stained with PI and annexin V-FITC. Data are presented as medians and interquartile ranges obtained from ten independent experiments. Mann-Whitney U test was used for statistical analysis. Flow cytometry analysis of the cell cycle (E-H). Representative figures of ten independent experiments are shown; numbers represent the procentages of cells in each phase of the cell cycle. Flow cytometry analysis of DNA fragmentation (TUNEL assay), (I-L). Representative figures of ten independent experiments are shown.

at $P<0.05$. Statistical analyses were carried out with the GraphPad Prism software version 4.0.

## Results

Here, we conducted the qualitative and quantitative studies of nuclear and cytoplasmic actin pools in cells undergoing mitotic catastrophe and apoptosis. To elicit a desired cell response, CHO AA8 cells lacking functional p53 were treated with increasing DOX doses (0.5, 1 and 2.5 $\mu$M).

Following DOX treatment, the presence of two different cell populations was revealed. One population consisted of flattened giant cells, several times bigger in size compared to control cells. We observed mononucleated giant cells, cells with lobulated nuclei or multiple nuclei of different sizes (Fig. 3E, F, I, J-L; Fig. 4C). Simultaneously, DOX induced formation of the CHO AA8 cells with apoptotic features (Fig. 3G, H; Fig. 4D). The number of shrunken cells that partially lost contact with the substratum increased together with increasing drug doses. The increase in DOX concentration correlated with the propensity of the giant cells towards micronucleation. Apart from the cells with typical apoptotic features and those with hallmarks of mitotic catastrophe, we observed the cells exhibiting extensive cytoplasmic vacuolization (Fig. 4B), indicative of autophagy. In some areas of CHO AA8 cells, particularly after treatment with higher DOX doses, we found severe changes within the cytoplasm and even debris. Interestingly, electron microscopic examination did not reveal the loss of nuclear membrane integrity (Fig. 4B).

*Annexin V-FITC/7-AAD assay*. After the DOX exposure, the marked decrease in number of viable CHO AA8 cells [Annexin V (-), 7-AAD (-)] was observed, compared to control cells (Fig. 1A). There was a slight increase in the percentage of Annexin V (+) 7-AAD (-) cells (Fig. 1B). In general, regardless of the dosage used, most of the DOX-treated cells were Annexin V (+) 7-AAD (+) or only 7-AAD (+) indicating late apoptosis or necrosis (Fig. 1C and D).

*TUNEL assay*. Together with increasing DOX doses we observed an increase in number of cells exhibiting DNA fragmentation (TUNEL-positive). The most significant difference was observed between control and samples treated with 2.5 $\mu$M DOX (Fig. 1L). Representative histograms show the effects of different DOX doses on cell cycle progression (Fig. 1E-H) and DNA fragmentation (Fig. 1I-L). We found positive correlation between DNA content and the occurrence of DNA breaks. Most TUNEL-positive cells were present among polyploid cells (DNA content of >4 n) (data not shown).

*Cell cycle analysis*. As shown in Fig. 1F-H, for CHO AA8 cells exposed to DOX, there was an increase in the number of

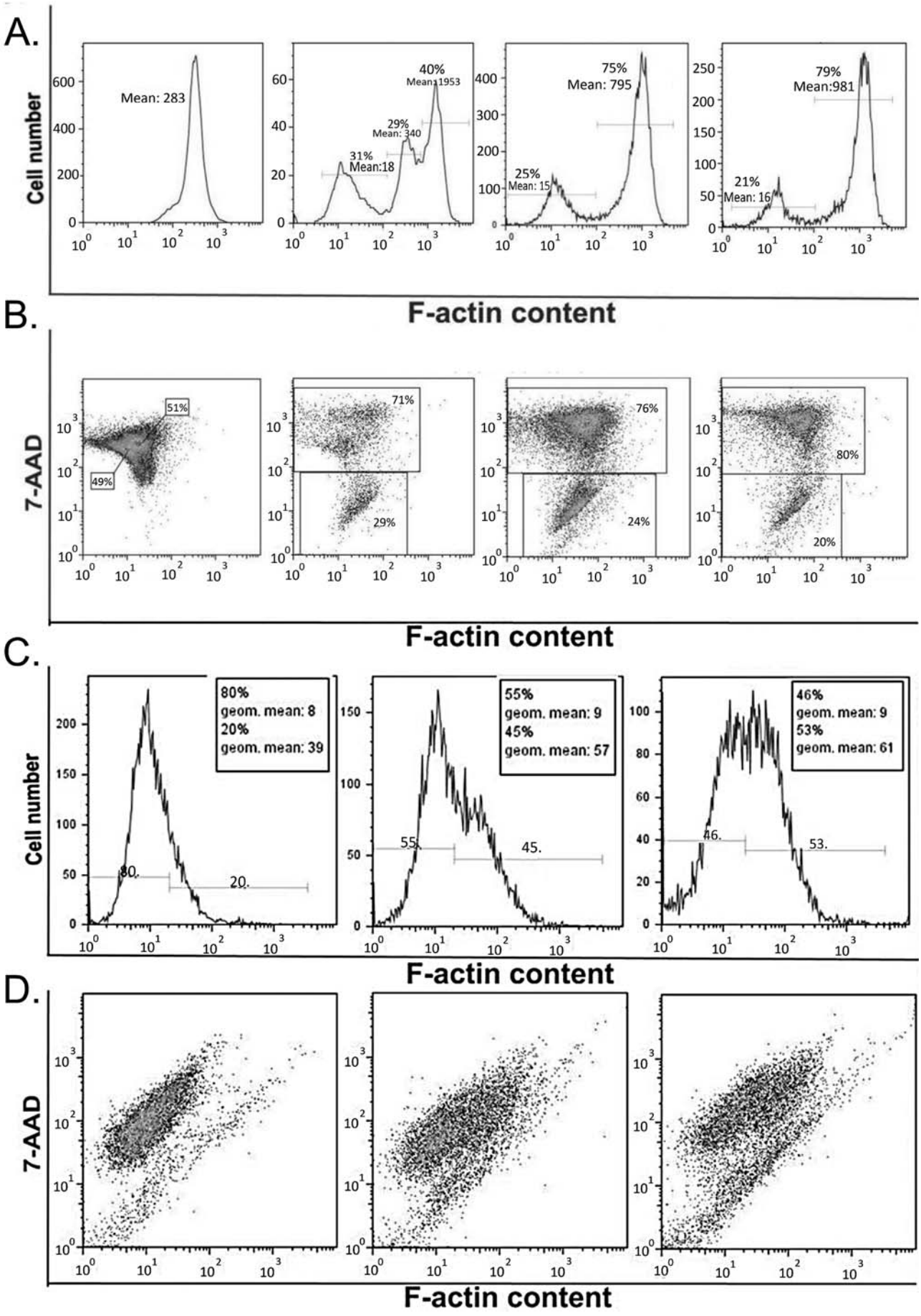


Figure 2. The cytometric analysis of F-actin content in the whole CHO AA8 cells (A). The relationship between nuclear DNA and F-actin content in the whole cells (B). The cytometric analysis of F-actin content in isolated nuclei (C). The relationship between nuclear DNA and F-actin content in the isolated nuclei (D). Representative figures of ten independent experiments are shown.

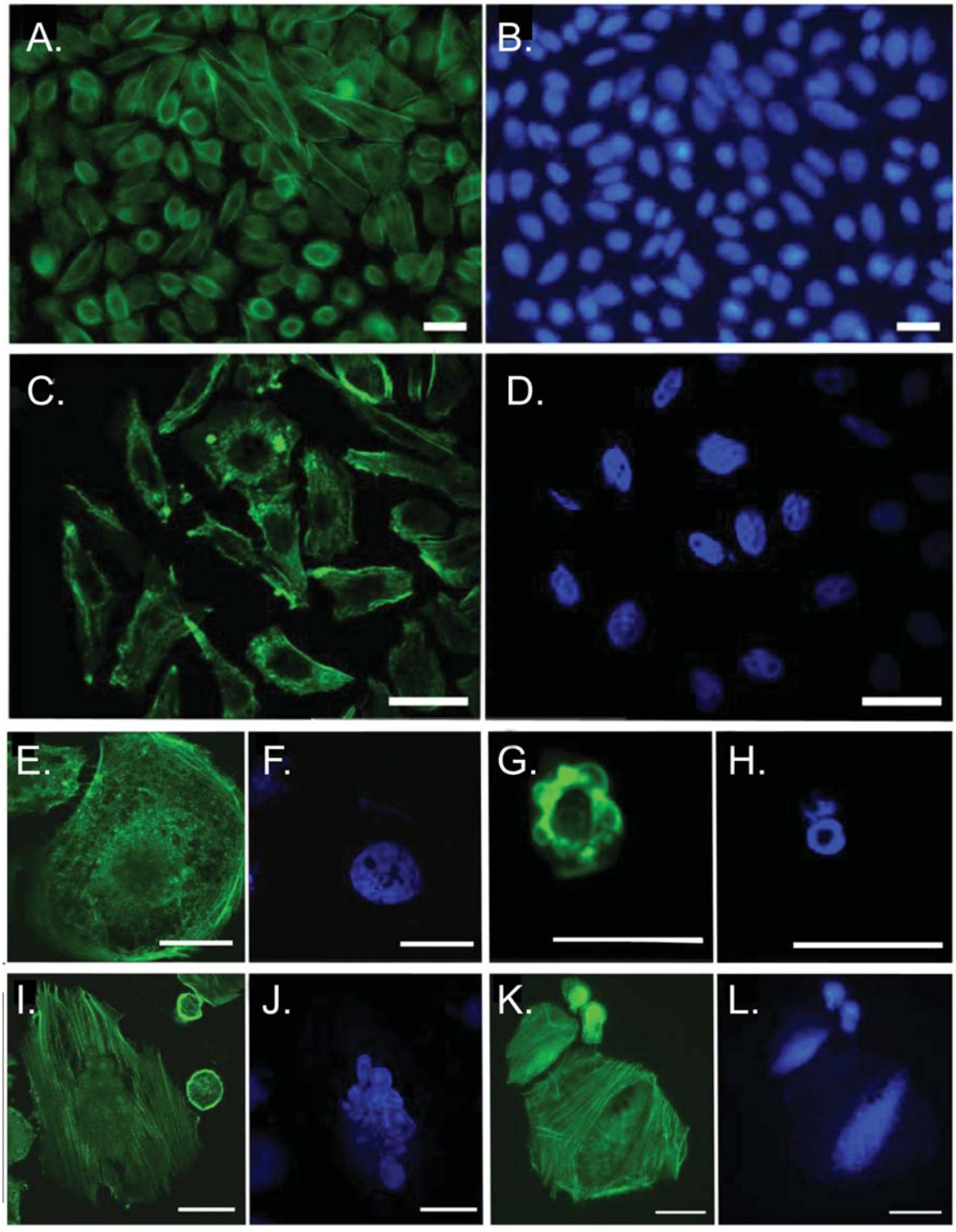


Figure 3. Conventional (A, B, K, L) and confocal (C-J) fluorescence microscopy analysis of F-actin distribution in CHO AA8 cells stained with phalloidin/Alexa Fluor 488 (A, C, E, G, I, K) and DAPI (B, D, F, H, J, L). Control cells (A-D), giant mononucleated (E, F) and multinucleated (I-L) cells with features of mitotic catstrophe and apoptotic cell (G, H) are shown after 0.5 $\mu$M (E, F), 1 $\mu$M (I, J) and 2.5 $\mu$M (G, H, K, L) DOX treatment. Bar, 20 $\mu$m.

polyploid cells that accumulated at the expense of cells in $G_1$/S. It was associated with the increase in sub-$G_1$ population, an indication of apoptosis.

*Fluorescence studies*. To assess F-actin distribution, conventional and confocal fluorescence microscopy were used. The images of control cells obtained from conventional microscope showed networks of peripheral microfilaments and arrays of actin stress fibres, typical for fibroblasts (Fig. 3A). After 0.5 $\mu$M DOX treatment, an overlapping pattern of staining of F-actin and nucleus was observed (Fig. 3E and F). Compared to control cells, multinucleated giant cells exhibited extended network of fine microfilaments with distinct bundles of F-actin and multiple stress fibers (Fig. 3I and K). Aside from the giant cells, exposure to 1 and 2.5 $\mu$M DOX caused in CHO AA8 cells hallmarks of apoptosis, including plasma membrane blebbing and DNA fragmentation. Chromatin of some apoptotic cells fragmented into multiple apoptotic

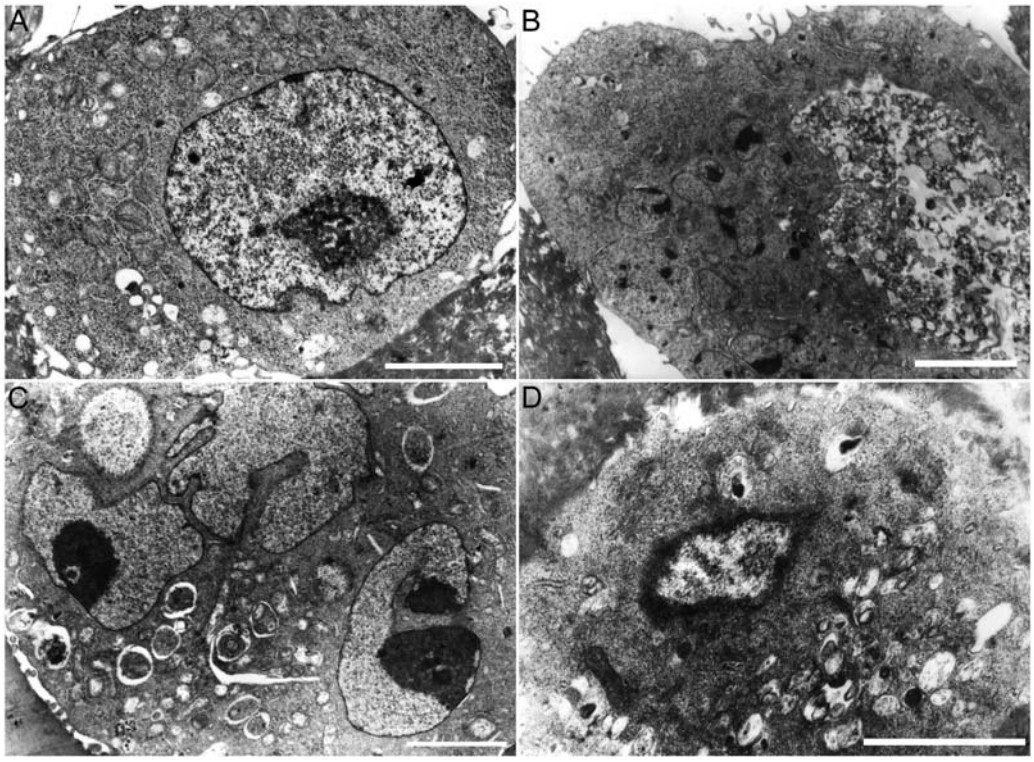


Figure 4. Electron micrographs of CHO AA8 cells treated with DOX. (A) Non-treated cell; oval-shaped nucleus with evenly dispersed chromatin, multiple mitochondria and electron-dense cytoplasm. Bar, 2 $\mu$m. (B) DOX 2.5 $\mu$M; micronuclei with electron-dense chromatin, intracellular area with vacuoles of different sizes and electron-dense material. Bar, 4 $\mu$m. (C) DOX 0.5 $\mu$M; similar to autophagic vacuoles with degraded material. Bar, 3 $\mu$m. (D) DOX 1 $\mu$M; nuclear shrinkage, chromatin margination. Bar, 2 $\mu$m.

bodies. We found positive staining of F-actin in apoptotic bodies (Fig. 3G) and DNA staining confirmed the chromatin presence in these structures (Fig. 3H). Bright staining of F-actin was also observed in non-fragmented nuclei of cells with apoptotic features (Fig. 3G). Merge of images showed correspondence of DNA and F-actin staining in the giant cells, both mononucleated and multinucleated (Fig. 3E, F, I-L). In the nuclear region of the giant cells, we found areas without DNA and F-actin staining similar to intranuclear cytoplasmic inclusions.

*Flow cytometric assay of F-actin content*. The cytometric analysis of F-actin content in CHO AA8 cells revealed its increase in response to DOX treatment. We observed positive correlation between F-actin content and DOX dosage (Fig. 2A) and between F-actin content and DNA staining (7-AAD) (Fig. 2B). In the case of isolated nuclei, loss of material during purification unabled us to receive reliable results at dose 2.5 $\mu$M DOX. At 0.5 $\mu$M and 1 $\mu$M DOX, we found an increase in F-actin content, depending on the dose used (Fig. 2C) and DNA content (Fig. 1D).

*Immunoelectron microscopic studies*. In order to confirm actin distribution in CHO AA8 cells, particularly in the nuclei, streptavidin-gold immunoelectron microscopical technique was used. In control and DOX-treated cells, positive immunogold labelling was observed both in the nuclei and the cytoplasm. Similar observations were made for the giant cells, however, the most intensive labelling was observed in chromatin clusters, within micronuclei (Fig. 5A). In mononucleated cells with chromatin margination, more immunogold particles were seen in areas of chromatin condensation than in the cytoplasm (Fig. 5B). In micronuclei of the giant cells, where chromatin clusters were not observed, particles for actin were evenly distributed and associated with heterochromatin (Fig. 5C). In the giant cells with intranuclear inclusions, immunogold particles were found within some of them (Fig. 5D). In control cells incubated with non-immune serum, positive labelling for F-actin was not found.

## Discussion

It has been widely proven, both *in vitro* (31-33) and *in vivo* (4), that DOX kills number of cell types via apoptosis. However, recent results have shown that this drug may trigger other cell response including senescence (7,34,35) and mitotic catastrophe (7,8,34). Although seemingly confusing, data presented in the cited papers clearly indicate dose-dependent mechanism of action of the drug. Low doses of DOX induced senescence and/or mitotic catastrophe whereas high doses caused apoptosis (7,8,36). Along the same line, following DOX treatment, we observed the occurrence of two cell populations; one consisted of the giant mono- and multinucleated cells typical of mitotic catastrophe (Fig. 3E, F, I-L) and the other with morphological features characteristic of autophagy or apoptosis (Fig. 3G, H; Fig. 4B). The former was more evident after incubation with 0.5 $\mu$M and 1 $\mu$M DOX, while 2.5 $\mu$M caused the appearance of cells with extensive micronucleation and multiple autophagic vacuoles. Together with increasing DOX doses, the loss of cytoplasmic membrane integrity was found as indicated in Annexin V/PI histogram (Fig. 1A-D). These results fully collaborated with

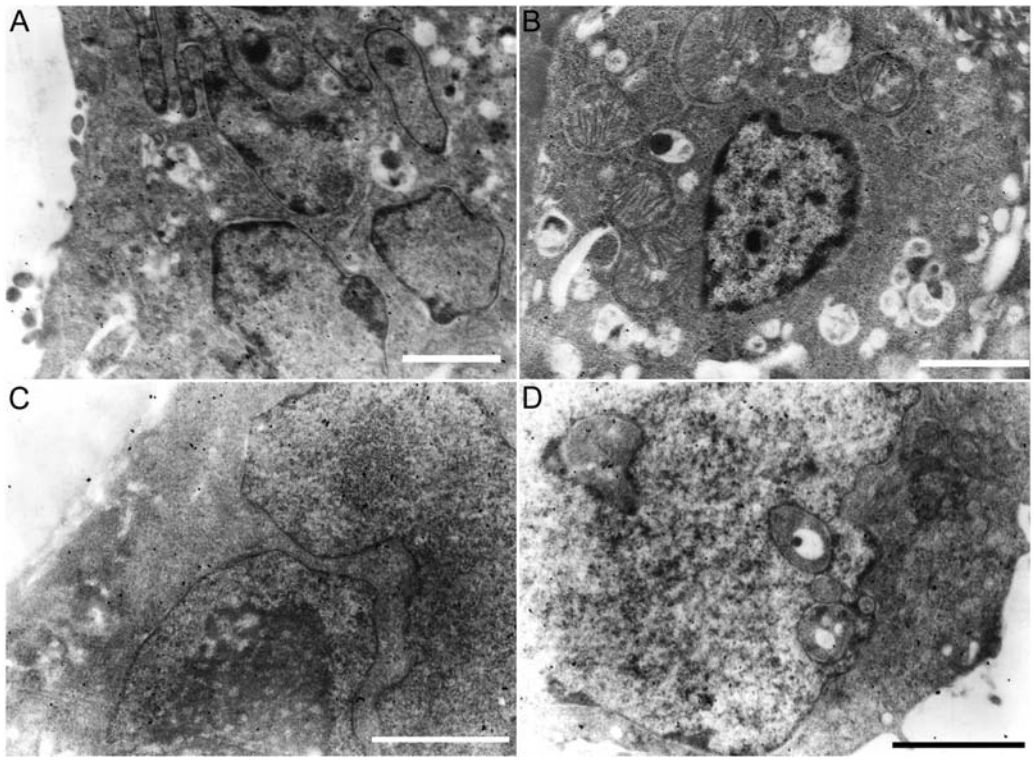


Figure 5. Immunolabelling of CHO AA8 cells treated with DOX. (A) DOX 1 $\mu$M; immunogold particles are localized in the areas of chromatin condensation within nuclei. Bar, 4 $\mu$m (B) DOX 2.5 $\mu$M; mononucleated CHO AA8 cell, immunogold particles are seen within marginated chromatin. Bar, 3 $\mu$m. (C) DOX 1 $\mu$M; immunogold particles are observed in the areas of condensed chromatin. Bar, 4 $\mu$m. (D) DOX 2.5 $\mu$M; CHO AA8 cell with cytoplasmic inclusions; in one of them, immunogold particles are seen. Bar, 2 $\mu$m.

DNA fragmentation studies that showed dose-dependence, with the greatest number of TUNEL-positive cells after treatment with 2.5 $\mu$M DOX (Fig. 1I-L). Similarly, after exposure to different DOX doses, Eom *et al* observed the occurrence of cells with abnormal nuclear morphologies indicative of mitotic catastrophe and shrunken, apoptotic cells. What is more, the authors showed that cells undergoing mitotic catastrophe were predominantly polyploid whereas apoptotic cells were mostly subdiploid (7). Our findings showed significant increase in hyperploid DNA content and slight increase in subdiploid cell population after treatment with all DOX doses (Fig. 1F-H). One of the possible explanations of the described phenomenon is that CHO AA8 cells used in this study, lack functional p53 (37) that is indispensable in many cell lines for DNA-damage induced apoptosis (33,38,39). Accumulating evidence suggests that p53-mutated cells with deficient cell cycle checkpoints are able to initiate endocycles without intervening cytokinesis that result in polyploidy and delayed cell death (13). What is more, the giant cells with multilobulated nuclei have been shown to arise not only from endocycling (13) but also from fusion of daughter cells (40,41).

Autophagy serves protective function in cells preventing them from entering apoptosis (14,42,43). It has been shown that autophagy inhibition may precipitate apoptosis (42). On the other hand, it is widely accepted that autophagy may develop into a separate type of cell death defined by extensive cytoplasmic vacuolization, lack of chromatin condensation and massive accumulation of autophagic vacuoles (14). Interestingly, recent studies have reported a kind of crosstalk between autophagic and apoptotic cell death and revealed that both processes may be simultaneously activated during cell death. According to the authors, autophagic and apoptotic pathways are closely connected and may be perceived as an integrated cell death mechanism (15,43). In our study, 2.5 $\mu$M DOX caused the appearance of cells with vacuoles, morphologically similar to autophagic vacuoles, containing cellular components. At the same time, we observed CHO AA8 cells with characteristic apoptotic features. It is explained that autophagy can serve as a 'fail-safe' mechanism (43); in certain conditions promoting survival and in others participating in cell death (43,44). Presumably, in our experimental conditions, the cells initiated pro-survival mechanism - autophagy that, because of irreversible damage, was followed by apoptosis, the results found by others (45,46).

Actin is a conserved cytoskeletal protein, distributed throughout the cell cytoplasm in monomeric (G-actin) and filamentous (F-actin) forms. In the present study, we found that following higher DOX doses CHO AA8 cells showed apoptotic features including chromatin fragmentation into apoptotic bodies. Notably, under our experimental conditions, positive staining of F-actin in the apoptotic bodies was evident (Fig. 3G). Similarly, Huot *et al* showed that in HUVEC cells treated with $H_2O_2$ actin underwent HSP27-mediated polymerization and accumulation at cell periphery and at the perimeter of the apoptotic blebs. The authors demonstrated that the already formed blebs contained large amount of HSP27 and indicated that actin polymerization was indispensable for plasma membrane blebbing (19). Analogous results were obtained by Levee *et al* who found that F-actin accumulated

in cell areas where apoptotic bodies were formed. The authors indicated that reorganization of F-actin network is fundamental for the proper formation of apoptotic bodies (20). What is more, Suarez-Huerta *et al* reported that during apoptosis in BAE cells F-actin underwent depolymerization (not proteolysis) followed by the recovery of microfilamentous network. Interestingly, actin filaments were observed at the basis of apoptotic bodies and the application of cytochalasin B or E prevented both membrane blebbing and development of apoptotic bodies. The authors have suggested that continuous actin reorganization is indispensable for maintaining the dynamic process of apoptotic body formation (47).

In our previous studies, we showed that, in HL-60 and K-562 cells undergoing apoptosis, actin is accumulated at sites of chromatin condensation and presumably involved in chromatin remodeling (24,48,49). Along the same line, following ultraviolet radiation, we observed apoptotic CHO AA8 cells exhibiting similar to above-mentioned actin reorganization pattern (6). In this study, DOX induced non-apoptotic cell response known as mitotic catastrophe, characterized by the occurrence of the giant multinucleated cells. Compared to control cells, the giant ones exhibited extended network of fine microfilaments, well organized bundles of F-actin and multiple stress fibers (Fig. 1M and O). The results showing that the actin cytoskeletal assembly was not inhibited suggest that essential cellular processes were not severely affected. Similarly, Hasinoff *et al* reported that CHO AA8 cells treated with dexrazoxane underwent multiple cycles of DNA replication without cytokinesis. As a result, multilobulated cells markedly increased in volume and ploidy occurred. Actin cytoskeleton was well-preserved (50). The results showing the existence of the undamaged network of actin and tubulin filaments in CHO AA8 cells undergoing mitotic catastrophe were demonstrated in our recent studies. We have revealed that hyperthermia and Taxol treatment resulted in appearance of the giant multinucleated CHO AA8 cells with the well organized network of fine filaments (51,52). In this study, we demonstrate not only the undamaged actin cytoskeleton in the undergoing mitotic catastrophe large cells but also the presence of actin in their multilobulated nuclei (Fig. 3E, I, K). To our knowledge we are the first to demonstrate this phenomenon. The observation was confirmed by fluorescence and electron microscopy, as well as flow cytometry analysis that revealed the increase in F-actin content following DOX treatment both in the whole cells and isolated nuclei. These data confirm previous reports (24,48,49) and provide further evidence for the role of actin in the process of cell death and chromatin organization.

It has been suggested that a pool of nuclear actin is mainly composed of G-actin (53). On the contrary, there are the studies reporting the presence of F-actin in nuclei (54-56). Nuclear F-actin was believed to be involved in virus replication in AcMNPV-infected IPLB-Sf-21 cells (56). Recently, it has been shown that in the nuclei of the living HeLa cells ≈20% of the total actin pool had properties of F-actin. The FRAP studies led the authors to discover only slight difference in equilibrium between globular and filamentous form, present in the cytoplasm and the nucleus. Moreover, the pool of nuclear F-actin turned over faster compared to the cytoplasmic actin pool (54). However, nuclear F-actin was unlikely to form filaments similar to that found in the cytoplasm (29). Ye *et al* convincingly demonstrated that polymeric actin in conjunction with nuclear myosin I is required for transcription, both *in vivo* and *in vitro* (57). Along the same line, nuclear F-actin was shown to participate in binding of p53 to the nuclear matrix that was increased after DNA damage. These results suggest the involvement of F-actin in p53-mediated cell response to DNA damaging factors (58). Based on observation of F-actin in the nuclei of the dying CHO AA8 cells, we hypothesize that this protein is involved in chromatin remodeling both in cells undergoing mitotic catastrophe and apoptosis.

In summary, our results demonstrate that DOX treatment led CHO AA8 cells to mitotic catastrophe that was followed by apoptosis with signs of autophagic vacuolization. Activation of cell death signaling pathway(s) correlated with the increase in F-actin content in the nucleus. We hypothesize that, in such cells, F-actin may be involved in chromatin remodeling. Further study is necessary to better understand the function of actin in the nuclei of dying cells. Taking into account that the cytoskeleton serves as a potential target in cancer therapy, the investigation of the relationship between actin reorganization and cell death seems particularly important.

## Acknowledgements

The study was supported by a grant from Ministry of Science and Higher Education No. 401224534.

## References

1. Hortobágyi GN: Anthracyclines in the treatment of cancer. An overview. Drugs 54: 1-7, 1997.
2. Gewirtz DA: A critical evaluation of the mechanisms of action proposed for the antitumor effects of the anthracycline antibiotics adriamycin and daunorubicin. Biochem Pharmacol 57: 727-741, 1999.
3. Mizutani H, Tada-Oikawa S, Hiraku Y, Kojima M and Kawanishi S: Mechanism of apoptosis induced by doxorubicin through the generation of hydrogen peroxide. Life Sci 76: 1439-1453, 2005.
4. Childs AC, Phaneuf SL, Dirks AJ, Phillips T and Leeuwenpburgh C: Doxorubicin treatment in vivo causes cytochrome C release and cardiomyocyte apoptosis, as well as increased mitochondrial efficiency, superoxide dismutase activity, and Bcl-2:Bax ratio. Cancer Res 62: 4592-4598, 2002.
5. Rebbaa A, Chou PM, Emran M and Mirkin BL: Doxorubicin-induced apoptosis in caspase-8-deficient neuroblastoma cells is mediated through direct action on mitochondria. Cancer Chemother Pharmacol 48: 423-428, 2001.
6. Grzanka D, Domaniewski J and Grzanka A: Effect of doxorubicin on actin reorganization in Chinese hamster ovary cells. Neoplasma 52: 46-51, 2005.
7. Eom YW, Kim MA, Park SS, *et al*: Two distinct modes of cell death induced by doxorubicin: apoptosis and cell death through mitotic catastrophe accompanied by senescence-like phenotype. Oncogene 24: 4765-4777, 2005.
8. Park SS, Eom YW and Choi KS: Cdc2 and Cdk2 play critical roles in low dose doxorubicin-induced cell death through mitotic catastrophe but not in high dose doxorubicin-induced apoptosis. Biochem Biophys Res Commun 334: 1014-1021, 2005.
9. Castedo M, Perfettini JL, Roumier T, Andreau K, Medema R and Kroemer G: Cell death by mitotic catastrophe: a molecular definition. Oncogene 23: 2825-2837, 2004.
10. Malorni W and Fiorentini C: Is the Rac GTPase-activating toxin CNF1 a smart hijacker of host cell fate? FASEB J 20: 606-609, 2006.
11. Nitta M, Kobayashi O, Honda S, *et al*: Spindle checkpoint function is required for mitotic catastrophe induced by DNA-damaging agents. Oncogene 23: 6548-6558, 2004.

ska A, Augustin E and Konopa J: Sequential induction of MOLT-4 cells by imidazoacridinone C-1311. Apoptosis 12: 2245-2257, 2007.
13. Erenpreisa J and Cragg MS: Mitotic death: a mechanism of survival? A review. Cancer Cell Int 1: 1, 2001.
14. Kroemer G, Galluzzi L, Vandenabeele P, *et al*: Classification of cell death: recommendations of the Nomenclature Committee on Cell Death 2009. Cell Death Differ 16: 3-11, 2009.
15. Thorburn A: Apoptosis and autophagy: regulatory connections between two supposedly different processes. Apoptosis 13: 1-9, 2008.
16. Hightower RC and Meagher RB: The molecular evolution of actin. Genetics 114: 315-332, 1986.
17. Carlier MF and Pantaloni D: Control of actin assembly dynamics in cell motility. J Biol Chem 282: 23005-23009, 2007.
18. White SR, Williams P, Wojcik KR, Sun S, Hiemstra PS, Rabe KF and Dorscheid DR: Initiation of apoptosis by actin cytoskeletal derangement in human airway epithelial cells. Am J Respir Cell Mol Biol 24: 282-294, 2001.
19. Huot J, Houle F, Rousseau S, Deschesnes RG, Shah GM and Landry J: SAPK2/p38-dependent F-actin reorganization regulates early membrane blebbing during stress-induced apoptosis. J Cell Biol 143: 1361-1373, 1998.
20. Levee MG, Dabrowska MI, Lelli JL Jr and Hinshaw DB: Actin polymerization and depolymerization during apoptosis in HL-60 cells. Am J Physiol 271: 1981-1992, 1996.
21. Bursch W, Hochegger K, Torok L, Marian B, Ellinger A and Hermann RS: Autophagic and apoptotic types of programmed cell death exhibit different fates of cytoskeletal filaments. J Cell Sci 113: 1189-1198, 2000.
22. Martin DN and Baehrecke EH: Caspases function in autophagic programmed cell death in Drosophila. Development 131: 275-284, 2004.
23. Croft DR, Coleman ML, Li S, Robertson D, Sullivan T, Stewart CL and Olson MF: Actin-myosin-based contraction is responsible for apoptotic nuclear disintegration. J Cell Biol 168: 245-255, 2005.
24. Grzanka A, Grzanka D and Orlikowska M: Fluorescence and ultrastructural localization of actin distribution patterns in the nucleus of HL-60 and K-562 cell lines treated with cytostatic drugs. Oncol Rep 11: 765-770, 2004.
25. Amankwah KS and De Boni U: Ultrastructural localization of filamentous actin within neuronal interphase nuclei in situ. Exp Cell Res 210: 315-325, 1994.
26. Milankov K and De Boni U: Cytochemical localization of actin and myosin aggregates in interphase nuclei in situ. Exp Cell Res 209: 189-199, 1993.
27. Sasseville AM and Langelier Y: In vitro interaction of the carboxy-terminal domain of lamin A with actin. FEBS Lett 425: 485-489, 1998.
28. Bettinger BT, Gilbert DM and Amberg DC: Actin up in the nucleus. Nat Rev Mol Cell Biol 5: 410-415, 2004.
29. Pederson T and Aebi U: Nuclear actin extends, with no contraction in sight. Mol Biol Cell 16: 5055-5060, 2005.
30. Percipalle P, Jonsson A, Nashchekin D, Karlsson C, Bergman T, Guialis A and Daneholt B: Nuclear actin is associated with a specific subset of hnRNP A/B-type proteins. Nucleic Acids Res 30: 1725-1734, 2002.
31. Gamen S, Anel A, Lasierra P, Alava MA, Martinez-Lorenzo MJ, Piñeiro A and Naval J: Doxorubicin-induced apoptosis in human T-cell leukemia is mediated by caspase-3 activation in a Fas-independent way. FEBS Lett 417: 360-364, 1997.
32. Kotamraju S, Konorev EA, Joseph J and Kalyanaraman B: Doxorubicin-induced apoptosis in endothelial cells and cardiomyocytes is ameliorated by nitrone spin traps and ebselen. Role of reactive oxygen and nitrogen species. J Biol Chem 275: 33585-33592, 2000.
33. Lorenzo E, Ruiz-Ruiz C, Quesada AJ, Hernández G, Rodríguez A, López-Rivas A and Redondo JM: Doxorubicin induces apoptosis and CD95 gene expression in human primary endothelial cells through a p53-dependent mechanism. J Biol Chem 277: 10883-10892, 2002.
34. Chang BD, Broude EV, Dokmanovic M, Zhu H, Ruth A, Xuan Y, Kandel ES, *et al*: A senescence-like phenotype distinguishes tumor cells that undergo terminal proliferation arrest after exposure to anticancer agents. Cancer Res 59: 3761-3767, 1999.
35. Rebbaa A, Zheng X, Chou PM and Mirkin BL: Caspase inhibition switches doxorubicin-induced apoptosis to senescence. Oncogene 22: 2805-2811, 2003.
36. Mansilla S, Priebe W and Portugal J: Transcriptional changes facilitate mitotic catastrophe in tumour cells that contain functional p53. Eur J Pharmacol 540: 34-45, 2006.
37. Johansson F, Lagerqvist A, Filippi S, Palitti F, Erixon K, Helleday T and Jenssen D: Caffeine delays replication fork progression and enhances UV-induced homologous recombination in Chinese hamster cell lines. DNA Repair 5: 1449-1458, 2006.
38. Lee JH, Lee E, Park J, Kim E, Kim J and Chung J: In vivo p53 function is indispensable for DNA damage-induced apoptotic signaling in Drosophila. FEBS Lett 550: 5-10, 2003.
39. Wang P, Yu J and Zhang L: The nuclear function of p53 is required for PUMA-mediated apoptosis induced by DNA damage. Proc Natl Acad Sci USA 104: 4054-4059, 2007.
40. Chu K, Teele N, Dewey MW, Albright N and Dewey WC: Computerized video time lapse study of cell cycle delay and arrest, mitotic catastrophe, apoptosis and clonogenic survival in irradiated 14-3-3sigma and CDKN1A (p21) knockout cell lines. Radiat Res 162: 270-286, 2004.
41. Erenpreisa J, Ivanov A, Wheatley SP, Kosmacek EA, Ianzini F, Anisimov AP and Mackey M: Endopolyploidy in irradiated p53-deficient tumour cell lines: persistence of cell division activity in giant cells expressing Aurora-B kinase. Cell Biol Int 32: 1044-1056, 2008.
42. Boya P, González-Polo RA, Casares N, Perfettini JL, Dessen P, Larochette N and Métivier D: Inhibition of macroautophagy triggers apoptosis. J Cell Sci 118: 3091-3102, 2005.
43. Kourtis N and Tavernarakis N: Autophagy and cell death in model organisms. Cell Death Differ 16: 21-30, 2009.
44. Bergmann A: Autophagy and cell death: no longer at odds. Cell 131: 1032-1034, 2007.
45. Abraham MC and Shaham S: Death without caspases, caspases without death. Trends Cell Biol 14: 184-193, 2004.
46. Kessel D: Promotion of PDT efficacy by a Bcl-2 antagonist. Photochem Photobiol 84: 809-814, 2008.
47. Suarez-Huerta N, Mosselmans R, Dumont JE and Robaye B: Actin depolymerization and polymerization are required during apoptosis in endothelial cells. J Cell Physiol 184: 239-245, 2000.
48. Grzanka A: Actin distribution patterns in HL-60 leukemia cells treated with etoposide. Acta Histochem 103: 453-464, 2001.
49. Grzanka A, Grzanka D and Orlikowska M: Cytoskeletal reorganization during process of apoptosis induced by cytostatic drugs in K-562 and HL-60 leukemia cell lines. Biochem Pharmacol 66: 1611-1617, 2003.
50. Hasinoff BB, Abram ME, Chee GL, Huebner E, Byard EH, Barnabé N and Ferrans VJ: The catalytic DNA topoisomerase II inhibitor dexrazoxane (ICRF-187) induces endopolyploidy in Chinese hamster ovary cells. J Pharmacol Exp Ther 295: 474-483, 2000.
51. Grzanka D, Stepien A, Grzanka A, Gackowska L, Helmin-Basa A and Szczepanski MA: Hyperthermia-induced reorganization of microtubules and microfilaments and cell killing in CHO AA8 cell line. Neoplasma 55: 409-415, 2008.
52. Stepien A, Grzanka A, Grzanka D, Andrzej Szczepanski M, Helmin-Basa A and Gackowska L: Taxol-induced polyploidy and cell death in CHO AA8 cells. Acta Histochem (In press).
53. Olave IA, Reck-Peterson SL and Crabtree GR: Nuclear actin and actin-related proteins in chromatin remodeling. Annu Rev Biochem 71: 755-781, 2002.
54. McDonald D, Carrero G, Andrin C, de Vries G and Hendzel MJ: Nucleoplasmic beta-actin exists in a dynamic equilibrium between low-mobility polymeric species and rapidly diffusing populations. J Cell Biol 172: 541-552, 2006.
55. Pederson T: As functional nuclear actin comes into view, is it globular, filamentous, or both? J Cell Biol 180: 1061-1064, 2008.
56. Volkman LE, Talhouk SN, Oppenheimer DI and Charlton CA: Nuclear F-actin: a functional component of baculovirus-infected lepidopteran cells? J Cell Sci 103: 15-22, 1992.
57. Ye J, Zhao J, Hoffmann-Rohrer U and Grummt I: Nuclear myosin I acts in concert with polymeric actin to drive RNA polymerase I transcription. Genes Dev 22: 322-330, 2008.
58. Okorokov AL, Rubbi CP, Metcalfe S and Milner J: The interaction of p53 with the nuclear matrix is mediated by F-actin and modulated by DNA damage. Oncogene 21: 356-367, 2002.